Electronic Supplementary Information

Monocrystalline NiS nanowire arrays supported by Ni foam as binder-free electrodes with outstanding performances

Yali Xu,[a, b] Weimin Du,[a*] Lulu Du,[a, c] Wenjuan Zhu,[a] Wei Guo,[a] Jingjing Chang,[a] Bing Zhang,[c] and Dehua Deng[a]

a. Henan Province Key Laboratory of New Optoelectronic Functional Materials, College of Chemistry and Chemical Engineering, Anyang Normal University, Anyang, Henan, 455002, P. R. China. E-mail: dwmchem@163.com; Fax: +86-372-290-0213; Tel: +86-372-290-0040

b. College of Chemistry and Molecular Engineering, Zhengzhou University, Zhengzhou, Henan, 450001, P. R. China.

c. School of Chemical Engineering and Energy, Zhengzhou University, Zhengzhou, Henan, 450001, China..

Synthesis of monocrystalline NiS nanowire arrays (NWAs) with high aspect ratio

All of reagents were analytical grade and were used without further purification. Via a simple hydrothermal method, monocrystalline NiS NWAs supported by Ni foam were prepared. Typically, A piece of Ni foam of 1 cm × 5 cm size was tread in hydrochloric acid for 45 min, and sequentially cleaned in ethanol and de-ionized water for 15 min, respectively. Besides, 1.8269 g thiourea was dissolved in pyridine by magnetic stirring until a homogeneous solution was formed. This solution was transferred into a 30 mL Teflon-lined stainless steel autoclave. A piece of pre-treated Ni foam was immersed in the solution followed by heating at 180℃ for 9 h. After the autoclave cooled to room temperature, monocrystalline NiS NWAs supported by Ni foam was obtained after washed with ethanol and distilled water several times, dried in a vacuum.

Material characterizations

X-ray diffraction (XRD, Rigaku Ultima III) equipped with a Cu Kα radiation source was used to characterize the crystal structures. The stereo surface morphologies, chemical composition and the element mapping images were captured by Scanning Electron Microscope (SEM, Hitachi, SU 8010) equipped with energy dispersive X-ray spectroscopy (EDX, Germany, Bruker Quantax). High-resolution transmission electron microscopy (HRTEM, FEI Tecnai F20 S-TWIN) was used to analyses the crystal lattice at an acceleration voltage of 200 kV.

Electrochemical Measurement

The electrochemical properties of monocrystalline NiS nano-arrays were studied in a three-electrode system with the electrolyte of 3 mol dm^{-3} KOH solution. A piece of platinum sheet was chosen as counter, and the saturated calomel electrode (SCE) was selected as the reference electrode. The cyclic voltammogram (CV) were measured by an electrochemical working station (CHI660E, Chenghua, Shanghai, China). The galvanostatic charge–discharge (GCD) and cycle stability were tested on an Arbin electrochemical instrument. Electrochemical impedance spectroscopy (EIS) analysis was conducted at open-circuit voltage in the frequency range of 100kHz to 0.01Hz

with AC voltage amplitude of 5mV using PARSTAT2273 advanced electrochemical system.

The specific capacitance from CV curves was calculated by using the Eqn. S1 as followed:

$$C_{sp} = \frac{1}{mv(V_c - V_a)} \int_{V_a}^{V_c} I(V)dV \qquad \text{(Eqn. S1)}$$

Where C ($F \cdot g^{-1}$), m (g), v($V \cdot s^{-1}$), Vc (V) and Va(V), and I (A) are the specific capacitance, the mass of the active materials in the electrode, scan rate, high and low potential limits of the CV tests, and the instant current on CV curves, respectively.

The areal/mass specific capacitance from GCD curves was calculated by using the Eqn. S2/S3 as followed:

$$C_A = I \times \Delta t/(S \times \Delta t) \qquad \text{(Eqn. S2)}$$

Where C_A ($F\ cm^{-2}$), I (A), Δt (s), S (cm^2) andΔV (V) are the areal capacitance, the discharge current, the discharge time, the work area of electrodes and the potential charge during discharge.

$$C = \frac{I \times \Delta t}{m \times \Delta v} \qquad \text{(Eqn. S3)}$$

where C ($F\ g^{-1}$) is the specific capacitance, I (A) is the discharge current, Δt (s) represents the discharge time, ΔV (V) is the potential change during discharge, and m (g) is the mass of the active material.

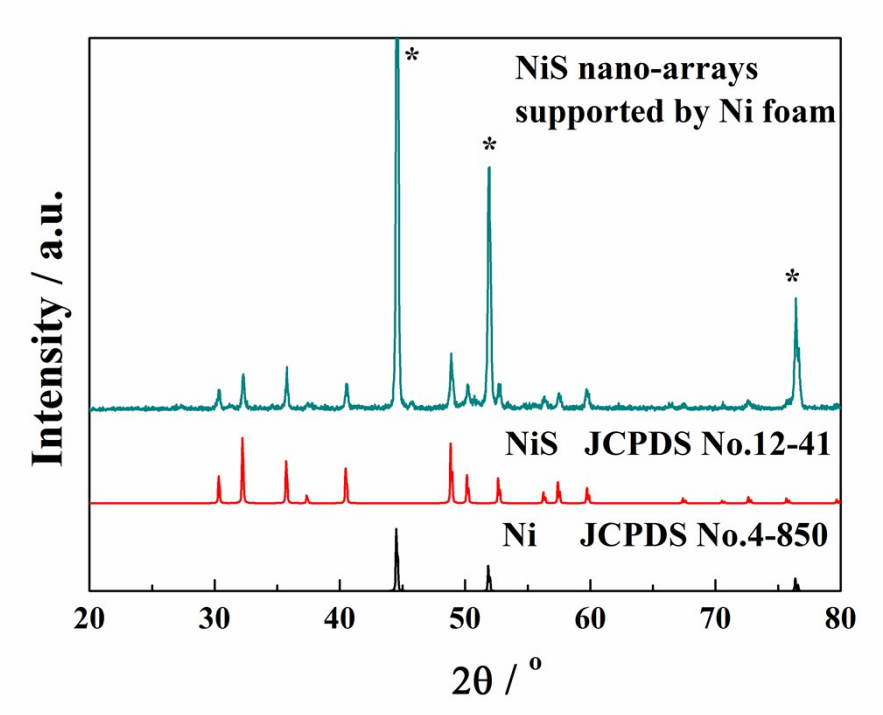

Fig. S1 XRD patterns of the NiS nanowire arrays supported by Ni foam

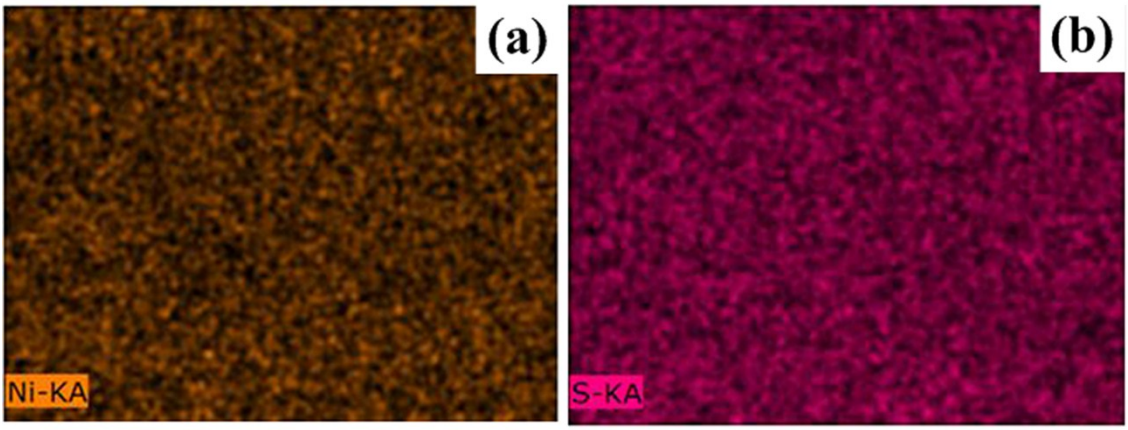

Fig. S2 Elemental mappings of Ni and S elements of NiS NWAs stripped from Ni foam

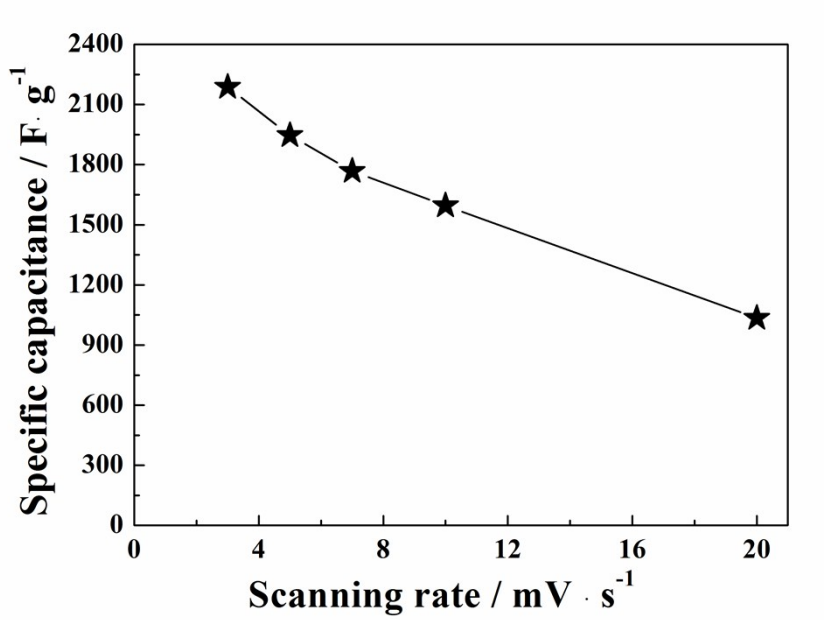

Fig. S3 Specific capacitance of NiS NWAs at different scanning rates.

Table. S1 Comparison of electrochemical performances of the present NiS NWAs with previously reported NiS nanostructures

Samples	Specific capacitance ($F\ g^{-1}$)	Current density ($A\ g^{-1}$)	Ref.
NiS/GO nanocomposite	800	1	S1
NiSnanospheres/rGO nanocomposite	1169	5	S2
NiS/rGO composite	628.12	2	S3
Hybrid NiS/CoOmesoporousnanosheet arrays on Ni foam	1054	6	S4
3D NiS-rGO hybrid nanostructure	852	2	S5
α- NiS NPs/CRs composites	946	2	S6
α- NiS hollow sphere	562.3	0.6	S7
Hierarchical flower-like β- NiS	857.76	2	S8
3D NiS dendritic arrays on Ni foam	404.1	2	S9
Porous NiSnanoflake arrays	718	2	S10
NiS hollow microspheres with mesoporous shells	1636.4	2	S11
NiS nanowire arrays	1456.7	3.33	**This work**

Table. S2 Comparison of electrochemical performances of the present NiS NWAs with previously reported other representative nanomaterials

Samples	Specific capacitance ($F\ g^{-1}$)	Current density ($A\ g^{-1}$)	Ref.
Swollen ammoniated MoS_2 nanostructure	296	3	S12
NiO nanosheet arrays on Ni foam	674.2	1	S13
AMC@$NiCo_2S_4$ nanostructure	636.3	2	S14
Hierarchical Co_3O_4@MnO_2 core-shell arrays on Ni foam	560	0.2	S15
MnO_2 nanotubes	365	0.25	S16

S1. A. Wang, H. Wang, S. Zhang, C. Mao, J. Song, H. Niu, B. Jin and Y. Tian, *Appl. Surf. Sci.*, 2013, **282**, 704-708.

S2. Z. Xing, Q. Chu, X. Ren, J. Tian, A. M. Asiri, K. A. Alamry, A. O. Al-Youbi and X. Sun, *Electrochem. Commun.*, 2013, **32**, 9-13.

S3. J. Yang, X. Duan, W. Guo, D. Li, H. Zhang and W. Zheng, *Nano Energy*, 2014, **5**, 74-81.

S4. J. Wu, C. Ouyang, S. Dou and S. Wang, *Nanotechnology*, 2015, **26**, 325401.

S5. F. Cai, R. Sun, Y. Kang, H. Chen, M. Chen and Q. Li, *RSC Adv.*, 2015, **5**, 23073-23079.

S6. C. Sun, M. Ma, J. Yang, Y. Zhang, P. Chen, W. Huang and X. Dong, *Sci. Rep.*, 2014, **4**, 7054-7059.

S7. C. Wei, C. Cheng, J. Zhao, Y. Wang, Y. Cheng, Y. Xu, W. Du and H. Pang, *Chemistry, an Asian journal*, 2015, **10**, 679-686.

S8. J. Yang, X. Duan, Q. Qin and W. Zheng, *J. Mater. Chem. A*, 2013, **1**, 7880-7884.

S9. Y. Zhang, J. Xu, Y. Zhang and X. Hu, *J. Mater. Sci: Mater. Electron.*, 2016, **27**, 8599-8605.

S10. X. Yan, X. Tong, L. Ma, Y. Tian, Y. Cai, C. Gong, M. Zhang and L. Liang, *Mater. Lett.*, 2014, **124**, 133-136.

S11. Z. Li, A. Gu, J. Sun and Q. Zhou, *New J. Chem.*, 2016, **40**, 1663-1670.

S12. D. Wang, Y. Xiao, X. Luo, Z. Wu, Y.-J. Wang and B. Fang, *ACS Sustainable Chem. Eng.*, 2017, **xxx**, xxx-xxx.

S13. M. Huang, F. Li, J. Y. Ji, Y. X. Zhang, X. L. Zhao and X. Gao, *CrystEngComm*, 2014, **16**, 2878-2884.

S14. T. Wang, Q. Le, G. Zhang, S. Zhu, B. Guan, J. Zhang, S. Xing and Y. Zhang, *Electrochim. Acta*, 2016, **211**, 627-635.

S15. M. Huang, Y. Zhang, F. Li, L. Zhang, Z. Wen and Q. Liu, *J. Power Sources*, 2014, **252**, 98-106.

S16. M. Huang, Y. Zhang, F. Li, L. Zhang, R. S. Ruoff, Z. Wen and Q. Liu, *Sci. Rep.*, 2014, **4**, 3878-3885.